J. Cent. South Univ. (2018) 25: 473−481
DOI: https://doi.org/10.1007/s11771-018-3751-6

Springer

Influence of heat treatment on microstructure and tribological properties of flame spraying Fe–Ni–Al alloy coating

Youcef Mouadji[1], Mohand Amokrane Bradai[2], Rassim Younes[2], Abdelhamid Sad-eddine[2], Abderrahim Benabbas[3]

1. National Polytechnic School of Constantine, Department of Mechanical Engineering, University of Constantine, Constantine 25000, Algeria;
2. Laboratory of Mechanics, Materials and Energetic, Faculty of Technology, University of Bejaia, Bejaia 06000, Algeria;
3. Laboratory Processes for Materials, Energy, Water and Environment, Faculty of Science and Technology, University of Bouira, Bouira 10000, Algeria

Abstract: The Fe-based coatings in powder form were deposited on a steel type E335 by flame spraying technique. The effects of the post heat treatment on the microstructure and the mechanical properties of sprayed coatings were studied. Post heat treatment was conducted in a furnace in air at 623 K, 823 K and 1023 K for 1 h and then cooled in air. The results showed that with the increase of annealing temperature, the microstructure of coating treated at 823 K and 1023 K had several changes as follows: the reduction of porosity, formation of carbides and oxides. It was found that the solid solution FCC (Fe, Ni), intermetallic compound $AlFe_3$ and carbides [Fe, C] were the main phases for coatings as-sprayed and treated at 623 K and while iron carbide, molybdenum carbide and oxide as Fe_3O_4 became the main phases and reinforced the solid solution FCC (Fe, Ni) phase for annealed coatings at 823 K. However, it was observed the disappearance of molybdenum carbide and oxide Fe_3O_4 at 1023 K. The coating annealed at 823 K exhibited an excellent wear resistance than the as-sprayed and annealed coatings at 623 K and 1023 K and shows the lower wear rate than another coating treated or as sprayed.

Key words: thermal spray; coatings; post heat treatment; microstructure; wear

Cite this article as: Youcef Mouadji, Mohand Amokrane Bradai, Rassim Younes, Abdelhamid Sad-eddine, Abderrahim Benabbas. Influence of heat treatment on microstructure and tribological properties of flame spraying Fe–Ni–Al alloy coating [J]. Journal of Central South University, 2018, 25(3): 473–481. DOI: https://doi.org/10.1007/s11771-018-3751-6.

1 Introduction

Thermal spraying is one kind of surface engineering technologies which is utilized in almost industrial fields. Continuous advancements and enhanced understanding of thermal spray technology have facilitated a synergetic approach towards a sustainable growth of its industrial applications [1–3]. Thermal spraying coatings deposited by techniques such as plasma spraying (PS), high velocity oxy-fuel (HVOF), arc wire, flame spraying, can provide a cost-effective solution for tribological application in rolling/sliding contact [4–7]. Post heat treatment is now widely used to further improve the required properties of coatings materials, such as furnace heat treatment [8–10], quenching [11] and laser remelting [12], among which furnace annealing is the most fundamental one. By adjusting the annealing temperature, it can reach the achievement of refining crystal, relieving residual stresses and even changing the microstructure and phases to enhance the mechanical properties [13], such as

Received date: 2016−12−27; **Accepted date:** 2017−12−20
Corresponding author: Rassim Younes, PhD; Tel: +213–34215105; Fax: +213–34215105; E-mail: rassimyounes@yahoo.fr; ORCID: 0000-0001-5422-1990

fracture toughness and wear resistance. However relative to bulkmaterials, little work has been done to analyze the effect of annealing on materials at small scale, such as films and coatings [14].

It has been found that the microstructure and characterization of the coatings were significantly affected by a post heat treatment [15]. As a result, the thermal fatigue behavior of the sintered coatings was greatly improved. The heat treatment of amorphous coatings leads to the precipitation of sub-micrometric crystals [16], which definitely enhances the mechanical properties of coatings, such as the microhardness, fracture toughness and wear resistance [17–20]. YOO et al [21] have found that the amorphous structured coatings exhibit a superior corrosion resistance to the crystallized coatings with high polarization resistance, and the corrosion resistance decreases after heat treatment. Studies on the post heat treatment of arc sprayed Fe-based amorphous coatings have not been reported so far, to the authors' knowledge.

The aim of this work is to study the effect of post heat treatments on the microstructure and tribological behavior of iron-based alloy coating produced by flame thermal spray process. The microstructural and structural characterization of the powder and coatings untreated and heat-treated at different temperatures 623 K, 823 K and 1023 K are obtained by using the scanning electron microscopy (SEM), energy dispersive spectroscopy (EDS) and XRD diffraction. Mechanical properties are investigated by determining the coefficient of friction and the wear rate of the coatings carried out under various applied loads.

2 Experimental

2.1 Preparation of coatings

The powder used was ProXon 21023 (denoted P23) based iron of granulometry (44–105 μm) and the nominal composition (Ni 22%; Al 17%; Mo 8%; C 0.16% and Fe balance) was used as sprayed material for its higher micro-hardness and better wear-resistance. The morphology of the powder is given in Figure 1.

The powder P23 was sprayed onto a grit blasted and degreased E335 with the chemical composition (wt%) obtained by using energy-dispersive X-ray fluorescence analysis (Fe (bal), Cu 0.2wt%, C (0.1–0.15)wt%, Ni <0.05wt%, Mn (0.2–0.25wt%). The process parameters were optimized as follows: The powders were flame sprayed onto grit blasted substrates using an oxygen-acetylene gun (model Castodyn DS 8000, Eutectic Castolin) and the input parameters were 400 kPa oxygen pressure, 70 kPa acetylene pressure and 350 kPa air pressure. In flame spraying, the powder materials were heated by an oxy-acetylene gas flame and heated particles were propelled onto the substrate by the expanding combustion gases. The corresponding spraying distance was 150 mm. The coatings subsequently deposited had an average thickness in the range of 800 μm. Heat treatment was carried in a C1228 cress single chamber heat treat furnace for 1 h. The temperature was selected at 623 K, 823 K and 1023 K. To avoid peeling off of the coating from the substrate due to larger thermal stresses, the heating and cooling of all samples were carried out in the furnace with low heating and cooling rate.

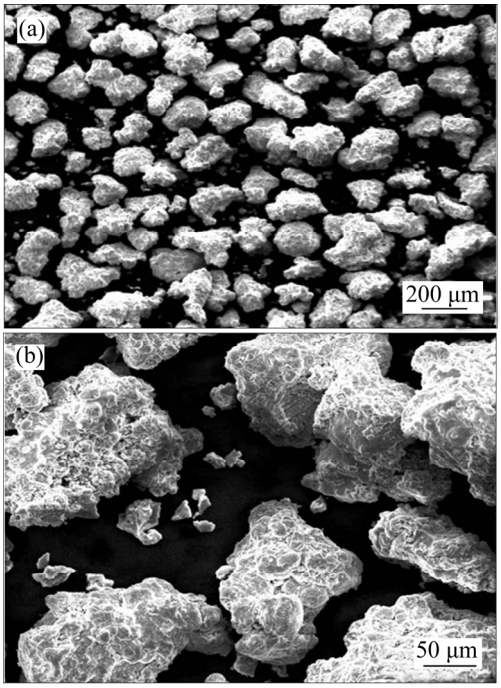

Figure 1 SEM images of powder Fe-based alloy

2.2 Microstructural and structural examination

The surface of samples was ground using SiC paper with grit sizes and finally polished with alumina. Microstructures of the initial powders and produced coatings were observed on their surface using an environmental scanning electronic microscope (ESEM) from Philips (FEI Quanta 200) in high vacuum. Chemical composition was analyzed using EDS. The phases present in the

powder and coatings untreated and post heat treated at different temperatures were identified using X-ray diffraction. The X-ray diffraction patterns were recorded at room temperature with a X'PERT PRO MRD diffractometer of PANalytical equipped with a Cu-anode X-ray tube and a curved graphite monochromator in the diffracted beam set of Cu-K_α radiation which includes the $K\alpha_1$ and $K\alpha_2$ wavelengths. The strong presence of defects in these materials creates a significant background noise; to improve counting statistics and increase the peak/background ratio, an acquisition time of 40 s was used per angular step of 0.04° over the 30°–120° (2θ) range. The identification of the crystal phases present in the coatings was performed using X'Pert HighScore software supported with the ICDD-PDF2 database.

2.3 Hardness investigation

The microhardness of the coatings (Vickers scale) was measured using a micro–Vickers hardness tester B 3212001 type Zwick. The measurements were carried out on the cross-sections of the coatings. A load of 300 g was selected for the average values of the coatings. The given microhardness value was the average of 10 measurements.

2.4 Wear resistance performance

The abrasive wear test was carried out on a pin-on-disc. The specimens dimensions were cylindrical pin of 10 mm diameter and 15 mm length. The pin-on-disc contact tests were performed under different loads (5, 10, 15, 20 and 30 N) with a siding distance of 900 m and sliding speed of 0.5 m/s. A sintered steel disc 100Cr6 was employed as the counter body with a new disc being used for each test. In order to study the wear behaviour of coatings in severe conditions, the tests were carried out without any lubrication. The wear experiencing by the samples during the tests was determined by weighing each sample before and after the test. The weight loss suffered by the pins was measured using electronic weighing balance having an accuracy of ±0.01 mg. The wear rate was calculated using the following equation:

$$K_v=\frac{\Delta m}{N_C} \tag{1}$$

where K_v is wear rate; Δm is mass loss; N_C is sliding distance.

The value of the static friction coefficient is obtained by the equation below:

$$\mu=\frac{F_t}{N} \tag{2}$$

where F_t is tangential force; N is normal force.

3 Results and discussions

3.1 XRD analysis

The XRD pattern of powder P23 is represented in Figure 2. The XRD pattern of powder P23 reveals three phases. The first one is a body-centered cubic (bcc) structure with a lattice parameter of 2.8849 Å that corresponds to the solid solution (JCPDS n° 00-047-1126) of the elements Fe, Ni, and Al. One can also note the presence of the (bcc) Fe-α which is practically pure (JCPDS No. 01-085-1410) corresponding to a parameter of 2.8849 Å. The third structure has monoclinic (JCPDS No. 01-078-0272). It corresponds to molybdenum iron carbide as (Fe, Mo)C. The XRD patterns of both the as-sprayed coatings and the treated coatings are shown in Figure 3. The diffraction X-ray patterns of the coatings as-sprayed and heat treated at 623 K (Figures 3(a) and (b)) revealed the presence of three common phases: The main phase is identified as face-centered cubic (FCC) (Fe, Ni) structure with a lattice parameter of 3.5160 Å that corresponds to the solid solution (JCPDS No. 00-003-1044). One can also note the presence of related FCC peaks corresponding to a parameter of 5.7934 Å with the intermetallic compound such as $AlFe_3$ (JCPDS No. 00-045-1203). The formation of this compound is made possible as a result of the larger content of

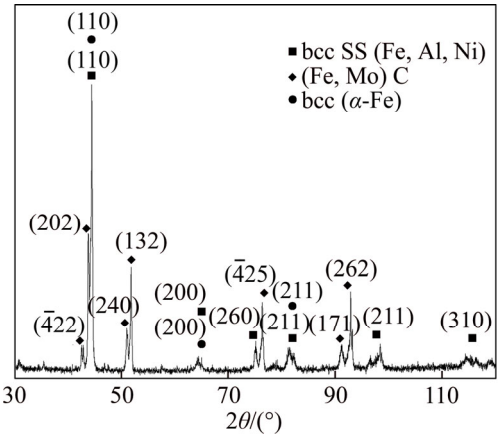

Figure 2 XRD pattern of P23 powder

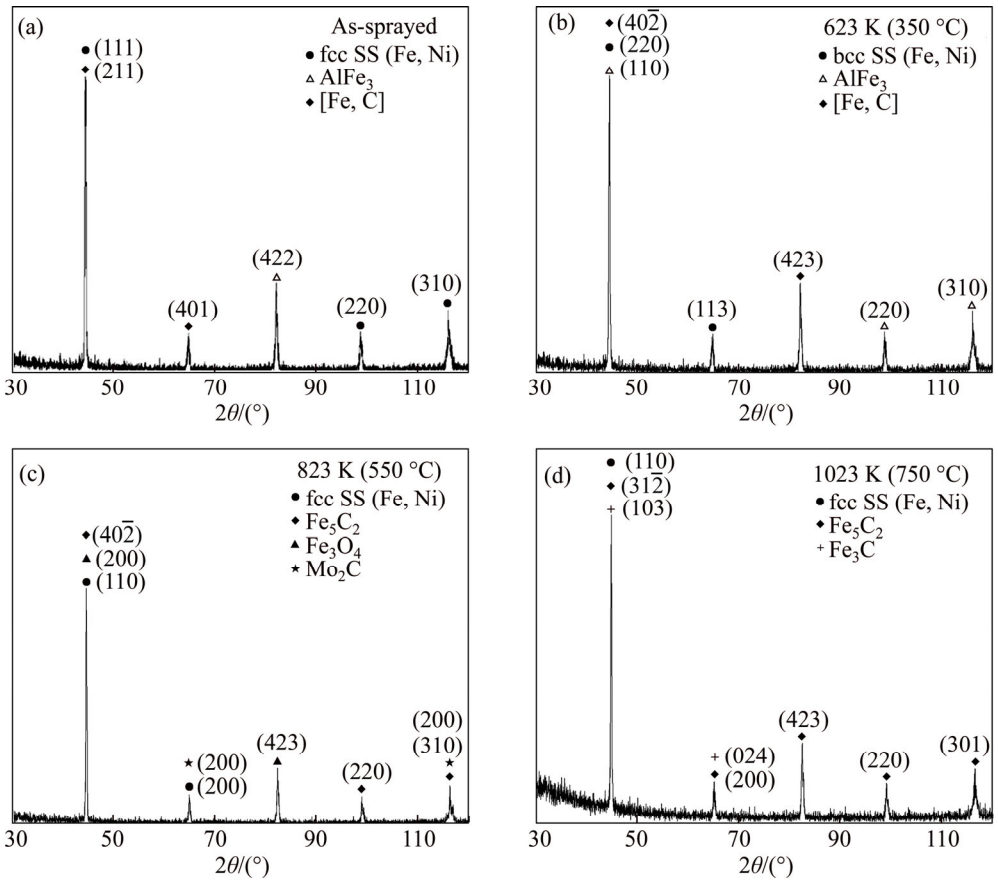

Figure 3 XRD patterns: (a) As-sprayed; (b) Treated at 623 K; (c) Treated at 823 K; (d) Treated at 1023 K

aluminum. The third structure corresponds to the carbide of iron (Fe, C) (JCPDS No. 00-017-0333). In this context, an important feature has to be underlined, dealing with the large statistical variations of composition. In contrary, the XRD pattern of the coating treated at 823 K (Figure 3(c)) revealed the disappearance of intermetallic phase AlFe3, only the FCC (Fe, Ni) solid solution is still present. One notes also the formation of others carbides type Fe_5C_2 (JCPDS No. 00-051-0997) and Mo_2C (JCPDS No. 001-1188) and a fraction of oxides such as Fe_3O_4 (JCPDS NO. 028-0491). After post heat treatment at 1023 K, the spectrum (Figure 3(d)) shows the presence of a FCC (Fe, Ni) solid solution while Mo dissolved in this solid solution and iron carbides type Fe_5C_2 and cementite Fe_3C (JCPDS No. 01-085-1317).

3.2 Microstructures of coatings

Microstructures of both the as-sprayed coatings and the treated coatings are shown in Figure 4. It is revealed that coatings are composed of numerous equiaxed structures, indicating that most particles were sprayed in the molten state or semi-molten when they impact. However, it is observed that there are more small dark precipitates in the coating as-sprayed. The modification of the coating's morphology is visible. Some original boundaries between thin lamellae get unclear, indicating that diffusion and sintering processes occurred during the heat treatment. The as sprayed coating has the highest porosity and decreased with increasing temperature of post heat treatment. Consequently, the microstructure of the coatings treated was densified. Typical microstructure of the as-sprayed coating (as shown in Figure 4(a)) consists of light phase and darker blocky phase which intercrosses each other and forms a kind of netlike structure and in agreement with the observation of ZHANG et al [22] and YOUNES et al [23].

Figures 4(a) and (b) reveal that the microstructure of the as-sprayed coatings and those treated at 623 K show three phases: the white area (A), the light grey area (B) and dark grey area (C). The results of EDS (as shown in Table1) indicated that the white area is relatively rich in Fe and contains a few of carbon element. The main phase

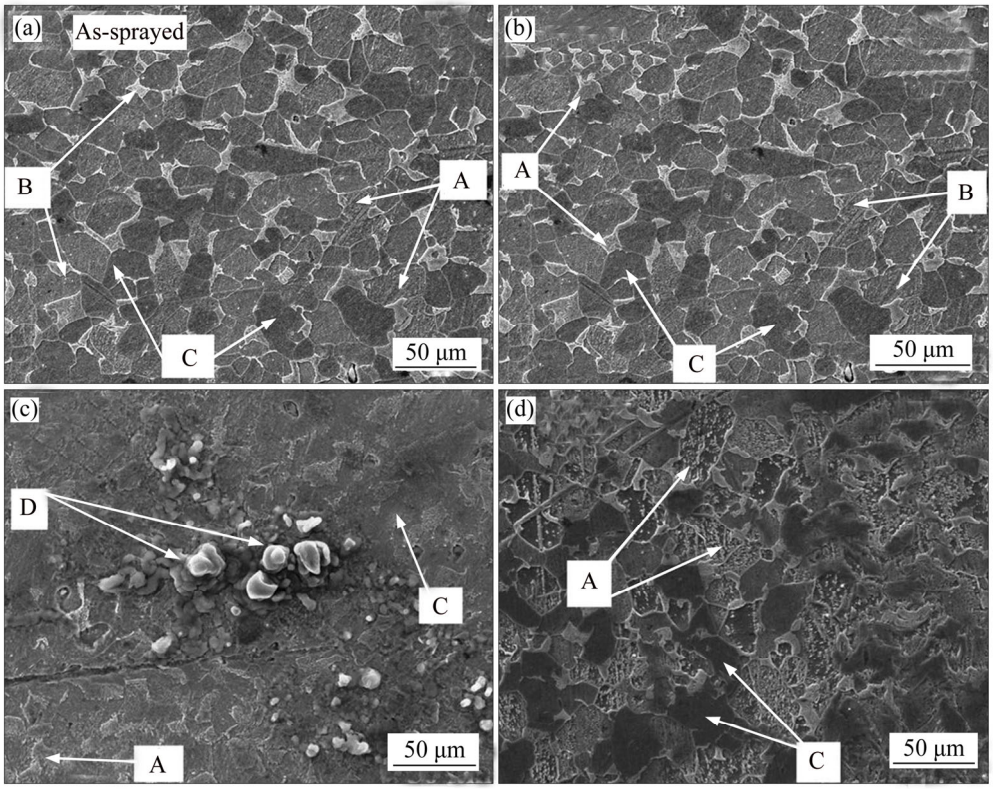

Figure 4 SEM images (backscattered electron) of coating P23: (a) As-sprayed; (b) Treated at 623 K; (c) Treated at 823 K; (d) Treated at 1023 K

of the dark area is identified as FCC (Fe, Ni) solid solution, while Mo dissolved in this solid solution and in light gray area formed intermetallic compound particles such as $AlFe_3$ as the XRD results proved. In contrary, the microstructure of the coating treated at 823 K has few pores. They find their origins probably in the trapping of air between the different coating layers. We also note the presence of white nodules that represent oxides type Fe_3O_4 (Figure 4(c), area (D)). These oxides have been demonstrated by microanalysis (EDS) while they are not noticed their presence in as-sprayed coating and heat treated at 623 K and 1023 K. In this coating, the intermetallic phase $AlFe_3$ has disappeared; only the FCC (Fe, Ni) solid solution and the carbides type Fe_5C_2 and Mo_2C are present (Table 1, white area (A)). Furthermore, the formation of these carbides is also revealed by the XRD diffraction. In flame spaying, the formation of hard films such as Fe_3O_4 oxide phase leads to improved wear properties [24, 25]. After post heat treatment at 1023 K, it can be seen in Figure 4(d) that the distribution of the darker area as FCC (Fe, Ni) solid solution is much more uniform while Mo and Al dissolved in this solid solution (Table 1, area (C)). In white area (A), more carbon took part in the reaction with iron which promoted the formation of iron carbide at the same time.

3.3 Measurements of Vickers hardness

Figure 5 shows that the substrate, coatings as-sprayed and heat treated at 623 K, 823 K and 1023 K have averages of hardness values of $HV_{0.2}(201\pm14)$, $HV_{0.2}(331\pm23)$, $HV_{0.2}(354\pm24)$, $HV_{0.2}(505\pm38)$ and $HV_{0.2}(453\pm31)$, respectively. The coatings heat-treated at 823 K show the highest hardness. The micro hardness of this coating is three times higher than that of antagonist substrate and nearly twice higher than that of coating as-sprayed and heat treated at 623 K which has an average $HV_{0.2}340$. This increased hardness is attributed to the fine microstructure formed by very compact and homogeneous strips and the presence of oxide Fe_3O_4 and carbides types Fe_5C_2 and Mo_2C, also contributed to increasing the wear resistance. On the other hand, the post heat treatment at 1023 K does not seem to affect the nature of the coating. Indeed, it records an average micro hardness of about $HV_{0.2}453$ which is practically the same as that of the coating treated at 823 K.

Table 1 Results of EDS test of different area in coatings

Coating	Area	*x*/%					
		Fe	Ni	Al	Mo	O	C
As-sprayed	White area (A)	72.08	—	—	1.53	—	26.13
	Light grey area (B)	71.08	—	23.13	—	1.93	—
	Dark grey area (C)	44.13	46.08	—	4.68	—	—
Coating treated at 623 K	White area (A)	69.08	—	—	3.53	—	27.13
	Light grey area (B)	77.08	—	21.13	—	—	—
	Dark grey area (C)	52.13	44.08	—	2.68	—	—
Coating treated at 823 K	White area (A)	49.08	5.53	—	30.09	—	15.13
	Dark grey area (C)	51.13	43.08	4.9	0.68	—	—
	Oxide (D)	56.57	—	—	—	43.43	—
Coating treated at 1023 K	White area (A)	79.08	3.53	—	0.4	—	17.13
	Dark grey area (C)	47.13	30.08	7.53	12.68	—	—

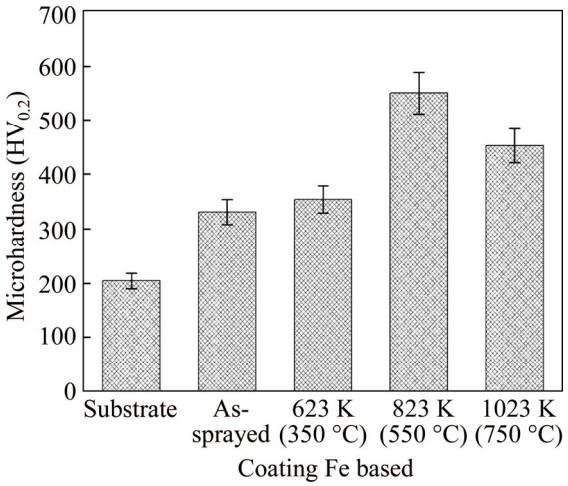

Figure 5 Hardness of coating Fe-based under 300 g

3.4 Wear property

Figure 6 shows that the coatings as-sprayed have a bad wear resistance with a high wear rate under sliding 0.5 m/s but the coatings thermally treated at 623 K and 1023 K led to decreasing slightly the wear rate. In contrast, the post heat treatment performed at 823 K exhibits better wear resistance. This is due to the fine microstrure formed by dense and compact strips and the presence of oxides Fe_3O_4 and carbide of molybdenum (Mo_2C) which has a highest micro hardness and often searched to reduce wear losses then wear rate.

Figure 7 shows that the friction coefficient of coatings as-sprayed and treated at different heat treatment have an average of 0.94 under a load of 5 N. Above this load, the coefficient of friction decreases in the same way as for coatings sprayed and treated at 623 K. However, this tendency is reversed for the heat treatment of 1023 K. This is due to the asperities that generate significant

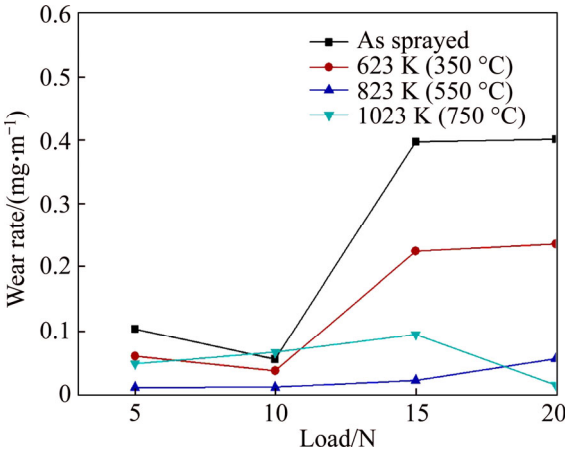

Figure 6 Wear rate of coatings P23 as-sprayed and heat treated in function of load

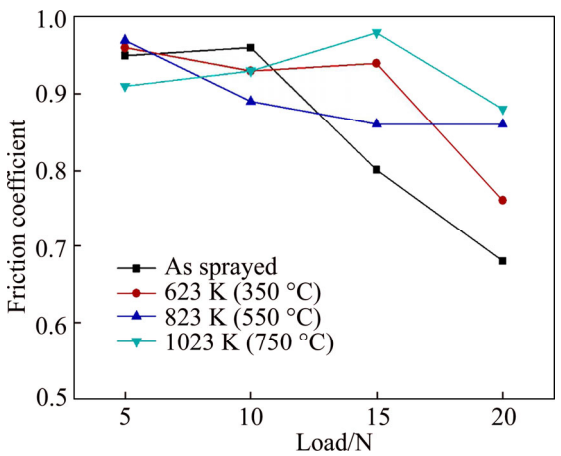

Figure 7 Friction coefficient of coatings P23 as-sprayed and heat treated in function of load

tangential force. On the other hand, the friction coefficient is stable during the test for the coating treated at 823 K. This is attributed to the fine microstructure formed by a large fraction of oxides and carbides which harden the multilayer involving the difficulty of removing of these layers. However, it is interesting to focus this study on the variation of the friction coefficient of coatings in function as sliding time for loads of 5 N and 20 N (Figure 8).

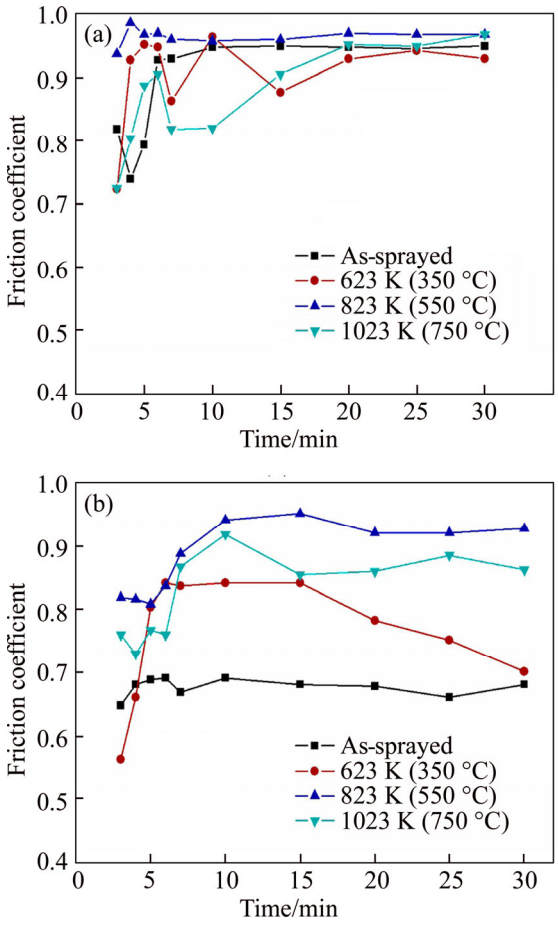

Figure 8 Friction coefficient of coatings P23 as-sprayed and heat treated in function of time: (a) 5 N; (b) 20 N

Figure 8 shows that the curves corresponding to the variation of the friction coefficient in function sliding time are nearly identical during the first 5 min under applied loads (5 N and 20 N). This transition phase can be explained by the presence of asperities which generate a tangential shear force near the normal force applied. After this phase, the coatings gave the same average friction coefficient about 0.92 under load 5 N for all samples (Figure 8(a)). When they slid under 20 N (Figure 8(b)), the less friction coefficient obtained (average 0.7) is from the coatings as-sprayed and treated at 623 K. One notes an important gap between others heat treated at 823 K and 1023 K. The coefficients of friction are stabilized at about 0.9. The highest friction coefficient is obtained from coating heat treated at 823 K. This is due to the presence of oxides type Fe_3O_4 while they are not noticed their presence in coatings as-sprayed and heat treated at 623 K and 1023 K. The formation of hard films such as Fe_3O_4 oxide phase leads to improved wear properties.

Through these results, we can conclude that the temperature of heat treatment for coatings affects the tribological properties. Indeed, the post heat treatment at 823 K stabilized the friction coefficient of coatings in function sliding time and increased their microhardness. On the other hand, the post heat treatment of the coatings at 623 K and 1023 K decreased the friction coefficient. From this, we can say clearly that the post heat treatment affects the mechanical properties of Fe-based coating.

4 Conclusions

In the present study, the effects of post heat treatment on the microstructure and the mechanical properties of flame sprayed coatings were investigated. The obtained results are summarized as follows:

1) Typical microstructure of the as-sprayed coating consists of blocky phases which intercrosses each other and forms a kind of netlike structure. However, the modification of the coating morphology is visible and had the higher porosity than another heat treated coating.

2) The microstructures of coatings treated at 823 K and 1023 K had several changes as follows: the reduction of porosity, formation of carbides and oxides. It was also found that the solid solution FCC (Fe, Ni), intermetallic compound $AlFe_3$ and carbides [Fe, C] were the main phases for coatings as-sprayed and treated at 623 K and while iron carbide, molybdenum carbide and oxide as Fe_3O_4 became the main phases and reinforced the solid solution FCC (Fe, Ni) phase for coatings annealed at 823 K. However, it was observed the disappearance of molybdenum carbide and oxide at 1023 K.

3) As the annealing temperature increases, the

coating shows a significant increase of Vickers hardness. The highest value of 505 HV could be obtained in the coating heat treated at 823 K.

4) The coatings annealed at 823 K exhibited a more excellent wear resistance than coatings as-sprayed and annealed at 623 K and 1023 K.

5) The best heat treatment is under temperature 823 K and it can be used to minimize the wear rate by enhancing various mechanical properties of coatings iron-base.

References

[1] FUJI M, YOSHIDA A, MAB J, SHIGEMURAC S, TANIC K. Rolling contact fatigue of alumina ceramics sprayed on steel roller under pure rolling contact condition [J]. Tribological International, 2006, 39: 856–862. DOI: https://doi.org/10.1016/j.triboint.2005.07.038.

[2] AHMED R. Contact fatigue failure modes of HVOF coatings [J] Wear, 2002, 253: 473–487. DOI: https://doi.org/10.1016/S0043-1648(02)00163-1.

[3] GAO Y, XU X, YAN Z, XIN G. High hardness alumina coatings prepared by low Power plasma spraying [J]. Surf Coat Technol, 2002, 154: 189–193. DOI: https://doi.org/10.1016/S0257-8972(01)01711-X.

[4] NIEMINEN R, VUORISTO P, NIEMI K, MANTYLA T, BARBEZAT G. Rolling contact fatigue failure mechanisms in plasma and HVOF sprayed WC-Co coatings [J]. Wear, 1997, 212: 66–77. DOI: https://doi.org/10.1016/S0043-1648(97)00138-5.

[5] STEWART S, AHMED R, ITSUKAICHI T. Contact fatigue failure evaluation of post-treated WC–NiCrBSi functionally graded thermal spray coatings [J]. Wear, 2004, 257: 962–983. DOI: https://doi.org/10.1016/j.wear.2004.05.008.

[6] NAKAJIMA A, MAWATARI T, YOSHIDA M, TANI K, NAKAHIRA A. Effects of coating thickness and slip ratio on durability of thermally sprayed WC cermet coating in rolling/sliding contact [J]. Wear, 2000, 241: 166–173. DOI: https://doi.org/10.1016/S0043-1648(00)00371-9.

[7] BRADAI M A, SAD-EDDINE A, MOUADJI Y, BENABBAS A, BOUNAR N, MAMMERI A. Microstructural and mechanical properties of Ni-base thermal spray coatings deposited by flame spraying [J]. Metall Mater Trans B, 2011, 42: 923–938.

[8] ZHANG Lei, DONG Xuan-pu, LI Ji-qiang, LI Kan, ZHANG Zong-kui, WANG Wen-jun, FAN Zi-tian. Microstructure evolution of Al-Si semi-solid slurry by gas bubble stirring method [J]. Journal of Central South University of Technology, 2011, 18: 1789–1794.

[9] PENG Z, SHANG Q, ZHANG Z, LU J. Microstructure and strengthening mechanism of Fe-based alloy powder cladding layer by plasma beam [J]. J Zhongyuan Univ Technol, 2007, 18(6): 6–9. (in Chinese)

[10] XIA Peng-cheng, YU Jing-jiang, SUN Xiao-feng, GUAN Heng-rong, HU Zhuang-qi. Influence of heat treatment on the microstructure and mechanical properties of DZ951 alloy [J]. Rare Met, 2008, 27 (2): 216–221.

[11] LI H, ZHAO G, HE L. Finite element method based simulation of stress-strain field in the quenching process [J]. Mater Sci Eng A, 2008, 478: 276–290. DOI: https://doi.org/10.1016/j.msea.2007.05.101.

[12] CHATTERJEE S, SHARIFF S M, PADMANABHAM G, MAJUMDAR J D, CHOUDHURY R A. Study on the effect of laser post-treatment on the properties of nano structured Al_2O_3–TiB_2–TiN based coatings developed by combined SHS and laser surface alloying [J]. Surf Coat Technol, 2010, 205(1): 131–138. DOI: https://doi.org/10.1016/j.surfcoat.2010.06.015.

[13] HAQUE M M, MALEQUE M A. Effect of process variables on structure and properties of aluminium–silicon piston alloy [J]. J Mater Process Technol, 1998, 77(1–3): 122–128. DOI: https://doi.org/10.1016/S0924-0136(97)00409-3.

[14] ZABIHI F, XIE Y, GAO S, ESLAMIAN M. Morphology, conductivity, and wetting characteristics of PEDOT:PSS thin films deposited by spin and spray coating, alloy [J]. App Surf Sci, 2015, 338: 163–177. DOI: https://doi.org/10.1016/j.apsusc.2015.02.128.

[15] CHOI S, CHO S, LEE J, JEONG D Y, KIM H. Reaction and interfacial structures between Ag paste with tellurite glass frits and Si wafer for solar cells [J]. Met Mater Inter, 2015, 21: 686–691.

[16] GARCIA C, ZHUKOV A, GONZALEZ J, ZHUKOVA V, VARGAD R, DEL VAL J J, LARIN V, BLANCO J M. Studies of structural and magnetic properties of glass-coated nanocrystalline $Fe_{79}Hf_7B_{12}Si_2$ microwires [J]. J Alloy Compd, 2006, 423: 116–119. DOI: https://doi.org/10.1016/j.jallcom.2005.12.029.

[17] PARK S Y, KIM M C, PARK C G. Mechanical properties and microstructure evolution of the nano WC–Co coatings fabricated by detonation gun spraying with post heat treatment [J]. Mater Sci Eng A, 2007, 450: 894–897. DOI: https://doi.org/10.1016/j.msea.2006.02.444.

[18] BOLLELI G, LUSVARGHI L. Heat treatment effects on the tribological performance of HVOF sprayed Co-Mo-Cr-Si coatings [J]. J Therm Spray Technol, 2006, 15(4): 802–810.

[19] BOLELLI G, LUSVARGHI L, BARLETTA M. HVOF-sprayed WC–CoCr coatings on Al alloy: Effect of the coating thickness on the tribological properties [J]. Wear, 2009, 267(5–8): 944–953. DOI: https://doi.org/10.1016/j.wear.2008.12.066.

[20] FERGUSON J B, SCHULTZ B F, VENUGOPALAN D, LOPEZ H F, ROHATGI P K. On the superposition of strengthening mechanisms in dispersion strengthened alloys and metal-matrix nanocomposites: Considerations of stress and energy [J]. Met Mater Inter, 2014, 20(2): 375–388.

[21] YOO Y H, LEE S H, KIM J G, KIM J S, LEE C. Effect of heat treatment on the corrosion resistance of Ni-based and Cu-based amorphous alloy coatings [J]. J Alloy Compd, 2008, 461(1, 2): 304–311. DOI: https://doi.org/10.1016/j.jallcom.2007.06.118.

[22] ZHANG S L, SUN X J, DONG H. Effect of deformation on the evolution of spheroidization for the ultra high carbon steel [J]. Mater Sci Eng A, 2007, 457: 319–324. DOI:

https://doi.org/10.1016/j.msea.2006.06.057.
[23] YOUNES R, BRADAI M A, SAD-EDDINE A, MOUADJI Y, BILEK A, BENABBAS. Microstructural and tribological properties of Al_2O_3-13pctTiO_2 thermal spray coatings deposited by flame spraying [J]. Metal Mater Trans B, 2015, 46(5): 2394–2403.
[24] CHO T Y, YOON J H, KIM S, SONG K O, JOO Y K, FANG W, ZHANG S H,YOUN S J, CHUN H G, HWANG S Y. A study on HVOF coatings of micron and nano WC–Co powders [J]. Surf Coat Technol, 2009, 203: 5556–5559. DOI: https://doi.org/10.1016/j.surfcoat.2008.06.106.
[25] TIAN W, WANG Y, YANG Y. Fretting wear behavior of conventional and nanostructured Al_2O_3–13 wt%TiO_2 coatings fabricated by plasma spray [J]. Wear, 2008 265: 1700–1707. DOI: https://doi.org/10.1016/j.wear.2008.04. 012.

(Edited by YANG Hua)

中文导读

热处理对火焰喷涂 Fe–Ni–Al 合金涂层组织和摩擦性能的影响

摘要：采用火焰喷涂技术在 E335 钢上制备粉末状 Fe 基涂层。研究了后续热处理对涂层组织和力学性能的影响。在 623 K、823 K 和 1023 K 的空气中对涂层进行后续热处理 1 h，然后随炉在空气中冷却。结果表明，随着退火温度的升高，823 K 和 1023 K 处理后涂层的微观结构发生了如下变化：孔隙率降低，碳化物和氧化物形成。在 623 K 时，涂层的主要相为固溶体 FCC(Fe，Ni)、金属间化合物 $AlFe_3$ 和碳化物[Fe，C]；碳化铁、碳化钼和氧化铁 Fe_3O_4 作为主要相增强了 823 K 退火涂层中的固溶体 FCC(Fe，Ni)相；但在 1023 K 处理涂层中观察到碳化钼和氧化物 Fe_3O_4 消失了。823 K 退火涂层的耐磨性优于 623 K 和 1023 K 退火涂层，其磨损率最低。

关键词：热喷涂；涂层；后续热处理；显微组织；磨损